ANALYSIS OF A HIGH-SPEED SQURREL CAGE INDUCTION MOTOR

Elena Zotova

Doctoral Degree Programme (1), FEEC BUT

E-mail: xzotov00@stud.feec.vutbr.cz

Supervised by: Ondřej Vítek

E-mail: viteko@feec.vutbr.cz

Abstract: This paper presents characteristics of a conventional three-phase two-pole high-speed induction motor designed for needs of woodworking applications with rated output power of 750W and synchronous rotational speed 24000 rpm. It was studied with analytical and numerical determination of high-speed motor parameters executed by means of software packages by ANSYS, afterward compared with the measured performances.

Keywords: High-speed, induction motor

1. INTRODUCTION

High-speed (HS) electrical machines nowadays may be required or become beneficial in various types of applications in which the need for high rotational speed to improve the work process is an inherent requirement and also presents the demand of lightness and compactness. The applications in which HS machines adopted are machine tools, spindle applications, compressors, vacuum pumps, turbine generators, electric-assisted turbochargers for car engines, flywheel energy storage systems, etc. [1], [2]. The most common types of HS machines used in industrial applications are the induction motor (IM) with a laminated and solid rotors and permanent magnet synchronous motor. The scope of this article covers only HS IMs. In general the IMs are adopted in HS applications because of its low maintenance, they are reliable, easily operated and noticed with relatively low cost, as well [3].

The design of HS motor has to reach the best compromise between the electromagnetic and mechanical constraints. The rotor of HS IM should be robust to meet the great stress due to the centrifugal forces at high rotational speeds. In addition to the robustness, the rotor should be electrically low loss because the heat generated in a rotor is difficult to be removed. This in its turn emphasizes the importance of thermal analysis in the design of HS machines. As with any kind of electrical machine, the cooling will determine the capacity limit of the HS IM.

In this paper the characteristics of a 2-pole HS induction motor designed for needs of woodworking applications are under consideration. It was studied with analytical and numerical determination of high-speed motor parameters, compared with the measured performance.

2. ANALITICAL AND NUMERICAL CALCULATIONS

The test motor was 3-phase 2-pole, 400 Hz, is done with a laminated magnetic core and an aluminum squirrel cage. The rated output power of the motor is 750W and rated speed is 23700 rpm. The rotor core material was M700-50A. Calculations performed at 400 Hz and at 200Hzs. The main parameters are given in Table 1.

Table 2, 3 and 4 present results of RMxprt computations and analytical calculations, for power supply frequencies 200 and 400 Hz supply voltage 115 and 230 Volts respectively, which are based on classical methods presented in [4] considering particular qualities of HS motor. As can be seen from the equation (1) when supply frequency and voltage vary, magnetic flux value remains unchanged and, consequently, magnetic flux density in stator and rotor yokes, in stator teeth and air gap remain unchanged as well.

$$\Phi = \frac{k_E \cdot U_1}{4{,}44 \cdot N_1 \cdot k_{v1} \cdot f_1}, \tag{1}$$

Rated output power [W]	375/750	Number of rotor slots	16
Rated frequency [Hz]	200/400	Outer diameter of the stator [mm]	75
Rated voltage [V]	115/230	Outer diameter of the rotor [mm]	38
Number of poles	2	Inner diameter of the stator [mm]	38,5
Number of phases	3	Air gap length [mm]	0,25
Turns per stator slot	28	Stator stack length [mm]	50
Number of stator slots	12		

Table 1: The main parameters of the studied IM.

For calculation of stator phase winding active resistance the copper resistivity was restated for the supposed temperature of copper (for 100 ° C). The same was done for resistivity of aluminum for determination of rotor cage and end-rings resistance. Reactances of stator and rotor windings were calculated for appropriate frequency.

	Calculation	RMxprt	Calculation	RMxprt
Frequency [Hz]	200		400	
Air gap magnetic flux density [T]	0,69	0,66	0,69	0,67
Stator yoke magnetic flux density [T]	1,34	1,22	1,34	1,24
Stator teeth magnetic flux density [T]	1,40	1,31	1,40	1,32
Rotor yoke magnetic flux density [T]	1,00	1,01	1,00	1,02
Rotor teeth magnetic flux density [T]	1,78	1,69	1,78	1,70
Core losses [W]	62,2	69,7	177,4	138
Mechanical losses [W]	41,0	100,1	100,5	353,4
Joule stator losses [W]	27,0	24,6	57,6	34
Joule rotor losses [W]	4,2	7,36	18,1	12,5
Total losses [W]	137,4	192,7	359,5	538

Table 2: Magnetic data and losses obtained by RMxprt and analytical calculations.

Armature core losses ΔP_{Fe} were determined by equation (2) considering required frequency of supply voltage, specific core loss at 1 T and 50 Hz [5]. Due to the magnetic flux density ripple in the air in the stator and rotor core arise stray losses which are the additional high frequency losses due to the stator and rotor slotting, they consist of surface core loss in the stator and in the rotor, and pulsation core loss in stator teeth and in rotor teeth (equation (3,5)).

$$\Delta P_{Fe} = \Delta p_{1/50} \cdot \left(\frac{f_1}{50}\right)^{4/3} \cdot \left[k_{adt} \cdot B_{1t}^2 \cdot m_{1t} + k_{ady} \cdot B_{1y}^2 \cdot m_{1y}\right], \tag{2}$$

where $k_{adt} > 1$ and $k_{ady} > 1$ are the factors accounting for the increase in losses due to metallurgical and manufacturing processes.

$$\Delta P_\delta = p_\delta \cdot (t_d - b_0) \cdot Q \cdot l_{Fe}, \tag{3}$$

where p_δ - the factor, that depends on surface manufacturing quality of the stator and the rotor.

$$p_\delta = 0{,}5 \cdot k_0 \cdot \left(\frac{Q \cdot n}{10000}\right)^{1{,}5} \cdot \left(b_0 \cdot t_d \cdot 10^3\right)^2, \tag{4}$$

$$\Delta P_p = 0{,}11 \cdot \left(\frac{Q \cdot n}{1000} \cdot B_p \right)^2 \cdot m_z, \tag{5}$$

where B_p - pulsation of the flux density in rotor tooth amplitude.

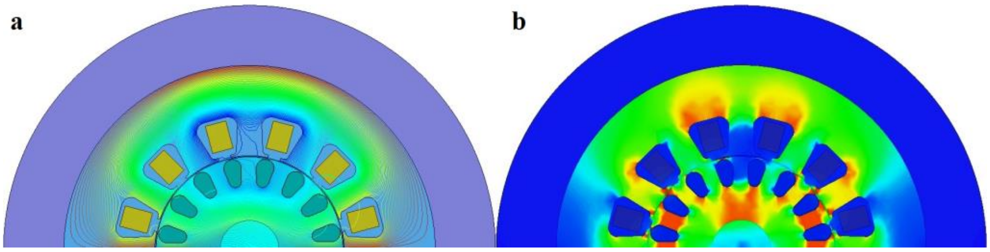

Figure 1: Flux lines (a) and flux line density (b) of the studied IM.

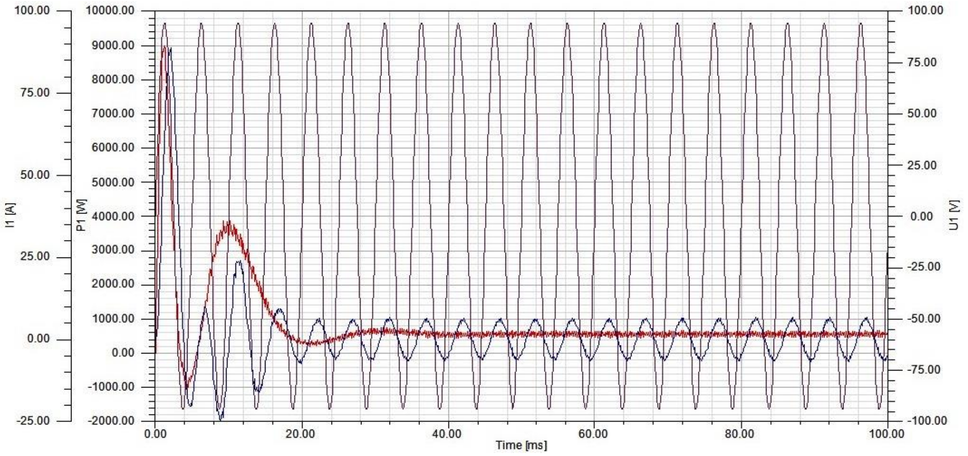

Figure 2: Current I_1, input voltage U_1 and Input power P_1 at 200Hz.

Mechanical losses were approximately determined as losses that include bearings frictional losses and windage losses that appear due to the friction between the rotating rotor and air. Bearings friction losses were restated according to maximal friction moment of the bearings and maximal mechanical angular speed by equations given on the website of bearings manufacturer. Calculation of the joule stator and rotor losses are based on the rated current in the stator and rotor and determined value of active resistance of stator and rotor windings.

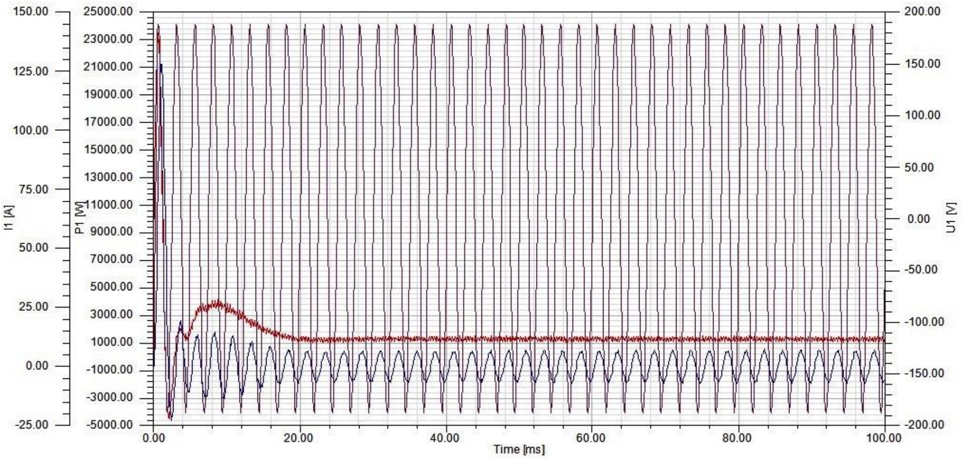

Figure 3: Current I_1, input voltage U_1 and Input power P_1 at 400Hz.

The determination of the motor characteristics were made using RMxprt Design software package by ANSYS for both frequencies and in the solution settings constant output power was adjusted to get all performance characteristics for nominal rotational speed and moving torque. Presumptive temperatures of working motor are 60°C and 100°C. Table 3 and 4 demonstrates obtained results. Then these results were used for following transient analysis by means of ANSYS Maxwell. Nonlinearity of the material (M700-50A) was set with B (H) curve [5]. A curve of specific losses from changes in the magnetic flux density at a certain frequency and the thickness of one steel plate was set for computation of losses due to eddy currents and hysteresis [5]. Aluminum and copper conductivities were restated for estimated temperatures of working IM.

The simulation was carried out taking into account the moment of inertia and the maximum load torque. As initial speed was set passport data idle speed of studied IM, which is 23900 rpm for 400 Hz and 11950 rpm for 200 Hz. Thus, transient responses, which occur at that very instant moment when the motor have been loaded, could be observed. Figures 1 (a) and 1 (b) demonstrate the flux lines and flux density distribution of the analyzed motor for 200 Hz respectively.

Figures 2 and 3 shows stator input voltage, current and power of working IM for frequences 200 and 400 Hz respectively. It can be seen current spike aimed to overcome the load torque after applying the load on the motor shaft, so slip increases, the rotor speed decreases. When transient responses are finished, speed increases again and average input powers and currents are P_1 = 558,4 W and I_1 = 4,3 A for 200 Hz, and P_1 = 1284,3 W and I_1 = 4,6 A for 400 Hz.

3. LABORATORY TESTS

The motor was tested at two supply frequencies. Figure 4 shows examined HS IM and the laboratory bench where measured motor connected with a dynamometer TorqueMaster of Magtrol SA company. The power inputs, voltages, currents, supply frequencies and power factors were metered by a digital power analyzer Yokogawa T 1800.

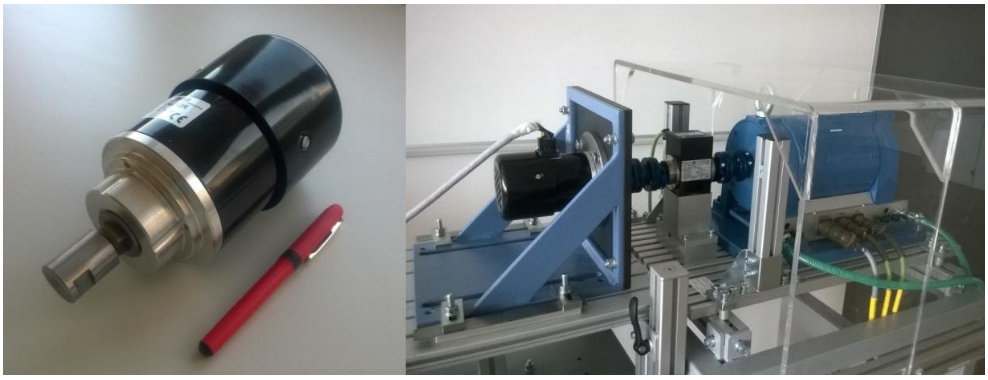

Figure 4: The 2-pole HS IM appearance and the laboratory bench for measuring.

HS_AM_750W	Calculation	RMXPRT	Maxwell	Test
Frequency [Hz]	200			
Moving speed [1/min]	11850	11817	11845,3	11840
Input phase voltage [V]	66,4	63	66,4	64,42
Stator phase current [A]	3,9	4,03	4,3	4,91
Input power [W]	512,4	567,7	558,4	575,3
Output power [W]	375	375	375,9	378,2
Losses [W]	137,4	192,7	182,5	197,1
Stranded loss [W]	27	24,5	28	38,6
Moving torque [Nm]	0,301	0,303	0,303	0,305
Efficiency [%]	73,2	66	67,3	66

Table 3: Comparation of main characteristics (200 Hz).

Tables 3 and 4 show experimantal results of the load test of the motor at both frequences and rated moving torques. The temperatures of the stator windings were measured by the traditional resistance method and they reach 60°C at 200 Hz and 100°C at 400 Hz. The winding resistances were measured by digital ohmmeter Cropico. It must be mentioned that motor worked in nominal conditions only about 10 minutes, so obtained resistances $R_{cu400} = 0{,}61\Omega$ and $R_{cu200} = 0{,}53\Omega$ which correspond to achieved temperatures are not maximal.

HS_AM_750W	Calculation	RMXPRT	Maxwell	Test
Frequency [Hz]	400			
Moving speed [1/min]	23700	23731,8	23786	23730
Input phase voltage [V]	132,8	132,8	132,8	136
Stator phase current [A]	5,7	4,5	4,58	5,29
Input power [W]	1110	1288,2	1280,6	1279,7
Output power [W]	750	750,2	747,3	743
Losses [W]	360	538	533,3	536,7
Stranded loss [W]	57,6	34	35,9	50,9
Moving torque [Nm]	0,301	0,301	0,3	0,299
Efficiency [%]	67,6	58,2	58,4	58

Table 4: Comparation of main characteristics (400 Hz).

Tables 3 and 4 shows the main perfomences of the motor obtained with analytical and computer calculations, FEM computer analysis and laboratory tests. Examination of the motor was carried out at rated frequency and at half of the rated frequency.

4. CONCLUSION

This paper shows the results of exploration of the conventional two-pole HS IM with a common squirrel cage rotor and rated power 750 W. The divergence between calculated results and laboratory tests, first of all, are because of the fact that in calculations losses caused by friction of the rotating parts of the motor with the air mass flow were not fully taken into account. It can be seen from the comparation of computed and experimental data, that these mechanical losses can be up to 35 % of the total losses and must be explored in more details in the analytical analysis. So examination of this motor was made for verification of the calculating methods and experience gained from the comparison and parsing of the resultes is being used for further study and design of HS motor with another rotor topologies typical for HS IM.

REFERENCES

[1] Zwyssig C., Kolar J.W. and Round S.D., “Megaspeed Drive Systems: Pushing Beyond 1 Million r/min”, IEEE/ASME Trans. on Mechatronics, Vol.14, No. 5, Oct. 2009, pp. 564–574.

[2] M. A. Rahman, A. Chiba, and T. Fukao, “Super high speed electrical machines—Summary,” in Proc. 2004 IEEE Power Eng. Soc. General Meeting, Jun. 6–10, vol. 2, pp. 1272–1275.

[3] Lähteenmäki J. Design and Voltage Supply of High-Speed Induction Machines, PhD thesis, Acta Polytechnica Scandinavica, Electrical Engineering Series, No 108, Espoo 2002. 140 p.

[4] Kopylov I. P.: Stavba elektrických strojů. 1. vydání Praha: Státní nakladatelství technické literatury; Moskva: Mir, 1988.

[5] ThyssenKrupp Steel AG, Power Core M700-50A/NGO electrical Steel, Oct. 2009, available: http://www.thyssenkrupp-steel-europe.com/tiny/kpj/download.pdf